No.

国立天文台 天文学データ解析計算センター
成果報告書 (平成 16 年度)

提出期限： 平成 17 年 3 月 14 日 (月)17:00 必着

応募カテゴリ（いずれかを選択） A
システム （いずれかを選択） VPP

プロジェクト ID: rmn12a

研究代表者（現在のユーザ ID：nogchims ）

氏名	野口 正史
所属機関名	東北大学大学院理学研究科天文学専攻
連絡先住所	〒 980-8578 仙台市青葉区荒巻字青葉 東北大学理学部天文学教室
電話番号	022-217-6507
E–mail	noguchi@astr.tohoku.ac.jp
職または学年	助教授
研究代表者が学生の場合には指導教官の氏名	

研究課題名

(和文)	銀河中心核による加熱が楕円銀河の化学力学進化に与える影響
(英文)	AGN heating and chemodynamical evolution of elliptical galaxies

研究分担者

氏名	所属機関名	E–mail	ユーザ ID
河田 大介	Centre for Astrophysics and Supercomputing, Swinburne University of Technology	dkawata@astro.swin.edu.au	kawatads
馬場 淳一	東北大学大学院理学研究科天文学専攻	baba@astr.tohoku.ac.jp	babajn

成果に関連して出版、もしくは印刷、投稿中の論文リスト

(1) このプロジェクト（同様の過去のプロジェクトも含む）での成果

今年度中に出版された論文、国際会議集録、国際会議、学会、研究会発表、その他出版物（印刷中、投稿中の場合はその旨を記載すること）

学術論文

河田 大介 & B.K. Gibson

Self-regulated active galactic nuclei heating in elliptical galaxies, 2005, MNRAS, 358L, 16

河田 大介, B.K. Gibson & R.A. Windhorst

Cosmological simulations of the high-redshift radio universe, 2004, MNRAS, 354, 387

研究会発表

河田 大介, B.K. Gibson & R.A. Windhorst

Cosmological simulations of the high-redshift radio universe, 理論懇シンポジウム, 東京大学, 2004 年 12 月

(2) これまでのプロジェクトの今年度中の成果

今年度中に出版された論文、国際会議集録、国際会議、学会、研究会発表、その他出版物（印刷中、投稿中の場合はその旨を記載すること）

※ 評価資料として利用いたしますので、様式・順序は任意ですが、学術論文については題名、著者、発行年月、雑誌名、巻、ページが記載されていること。

特になし。

成果の概要

Abstract

We study the effect of active galactic nuclei (AGN) heating on the chemodynamical evolution of elliptical galaxies and their X-ray and optical properties using high-resolution Λ-dominated cold dark matter cosmological simulations. Our model considers an AGN as being "active" when a convergent gas inflow condition exists within a galaxy's nucleus; otherwise, the AGN is assumed to remain dormant. This induces a self-regulated activity for the AGN, the result of which leads to a stable hot corona and the suppression of significant late-time star formation - characteristics not encountered in traditional chemodynamical models of ellipticals. These properties of our AGN heating model leads to a system consistent with both the X-ray and optical properties of comparable elliptical galaxies.

1. Introduction

One of the primary science drivers for the next generation of ground- and space-based observational facilities which spread over multi-wavelength is an understanding of the physics of galaxy formation and evolution. In the case of elliptical galaxies, the optical regime provides constraints on the properties of the underlying stellar populations, while the X-ray regime yields insights into the physical conditions of the associated hot interstellar (coronal) medium.

Kawata & Gibson (2003b, KG03b) presented a first attempt at explaining both the X-ray and optical properties of ellipticals via the use of self-consistent cosmological simulations.

Using a standard "recipe" for galaxy formation, they found that radiative cooling is important to interpret the observed X-ray luminosity (L_X), temperature (T_X), and metallicity ($[Fe/H]_X$) of the hot gas of elliptical galaxies. However, these models were subject to an unavoidable serious problem, in that the cooled gas unavoidably led to excessive star formation at low redshift (see also Suginohara & Ostriker , 1998; Tornatore et al. , 2003). This late-time star formation led to associated stellar populations which were too blue with respect to observations.

KG03b suggested that a heating mechanism not included in their simulations would be required to suppress this enhanced cooling and consequent star formation. In this paper, we examine one such potential mechanism - heating by an active galactic nucleus (AGN). In such a picture, one might expect an AGN could become "active" only when being fed "fuel" - i.e., when cold gas inflows into the central region, the AGN would activate and heat the surrounding gas, and potentially balance the associated radiative cooling (e.g. Churazov et al. , 2002). Once the infalling fuel source is quenched by the AGN heating, the AGN reverts to its quiescent state, and cycle can begin anew. This self-regulation provides heating (suppressing star formation) without compromising cooling (required to recover the empirical X-ray properties). Recent high-resolution X-ray images taken by *Chandra* reveal that the central hot gas of ellipticals is not smoothly distributed, but possesses cavities on scales comparable to the radio emission (e.g. Böhringer et al. , 1993). The X-ray holes are also seen on the cluster scale (> 50 kpc), and are often coincident with extended radio lobes (e.g. McNamara et al. , 2000; Fujita et al. , 2002). These features are considered to be a relic of the influence of AGN activity upon the hot gas in ellipticals and clusters (Churazov et al. , 2001).

Our current study examines the effect of AGN heating on both the optical *and* X-ray properties of giant elliptical galaxies in the context of a self-consistent treatment of cosmological evolution. Several earlier studies of the effect of AGN heating on the hot gas of ellipticals can be seen in Binney & Tabor (1995); Churazov et al. (2001); Ciotti & Ostriker (2001). While all important contributions to the field, these previous studies were (a) restricted in their temporal coverage to <15% of a Hubble time, and (b) did not trace star formation or mass accretion self-consistently within a Λ-dominated cold dark matter (ΛCDM) cosmology. Our cosmological simulation makes it possible to investigate whether or not AGN heating can lead to (a) a stable condition for the hot gas, and (b) suppress late-time star formation.

2. Methods

Our simulations were carried out using the galactic chemodynamics code `GCD+` (Kawata & Gibson , 2003a) with initial conditions identical to those described in KG03b. `GCD+` is a three-dimensional tree N-body/smoothed particle hydrodynamics (SPH) code which incorporates self-gravity, hydrodynamics, radiative cooling, star formation, supernovae (SNe) feedback, and metal enrichment. `GCD+` takes account of the chemical enrichment by both Type II (SNe II) and Type Ia (SNe Ia) SNe, mass-loss from intermediate mass stars, and follows the chemical enrichment history of both the stellar and gas components of the system. Here, we briefly describe our cosmological simulation models.

We adopt a ΛCDM cosmology (Ω_0=0.3, Λ_0=0.7, Ω_b=0.019h^{-2}, h=0.7, and σ_8=0.9) and use a multi-resolution technique to achieve high-resolution in the regions of interest, including the tidal forces from neighbouring large-scale structures. The initial conditions for the simulations

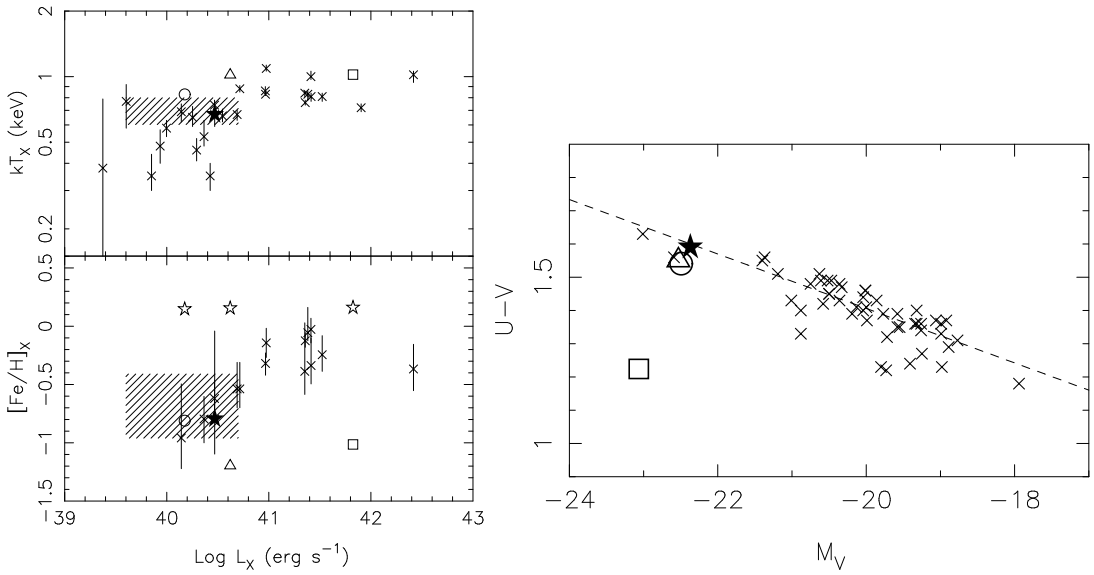

Fig. 1: *Left*: Comparison of the simulated and observed (crosses with error bars) $L_X - T_X$ relations (upper) and $[Fe/H]_X - L_X$ relations (lower). The square/circle/triangle indicates the predictions of Model 1/2/2L. Open stars in the lower panel show the predicted mean metallicity of the stellar component for the two models. The observational data are from MOM00. The shaded area represents the range of L_X and T_X for a sample of elliptical galaxies with low-L_X and high-T_X (group 5 in MOM00), and 90 % confidence limit of $[Fe/H]_X$ from the composite X-ray spectrum of these galaxies. *Right*: Comparison of the simulated $U - V$ CMR (square/circle/triagle for Models 1/2/2L, respectively) and that of the Coma cluster ellipticals (crosses). The observational data are from Bower, Lucey & Ellis (1992). The dashed line shows the CMR fitted to the Coma Cluster galaxies. The solid star corresponds to one of these galaxies, NGC 3923 whose total magnitude is obtained from de Vaucouleurs et al. (1991), and colours are from Persson, Frogel & Aaronson (1979) who presented the colours within a aperture similar in size to what Bower, Lucey & Ellis (1992).

are constructed using the public software `GRAFIC2` (Bertschinger , 2001). Gas dynamics and star formation are included only within the relevant high-resolution region (∼12 Mpc at z=0); the surrounding low-resolution region (∼43 Mpc) contributes to the high-resolution region only through gravity. Consequently, the initial condition consists of total 190093 dark matter particles and 134336 gas particles. The mass and softening length of individual gas (dark matter) particles in the high-resolution region are 5.86×10^7 (3.95×10^8) $M_\odot$ and 2.27 (4.29) kpc, respectively. KG03b found an appropriate elliptical galaxy analog in the high-resolution region, which acts as the focus for this study. The total virial mass of this galaxy is 2×10^{13} $M_\odot$. The target galaxy is relatively isolated, with only a few low-mass satellites remaining at z=0. Fig. 1 of KG03b shows the morphological evolution of dark matter in the simulation volume and the evolution of the stellar component of the target galaxy. The galaxy forms through conventional hierarchical clustering between redshifts z=3 and z=1. The morphology has not changed dramatically since z=1.

KG03b presented the results of three different radiative cooling and SNe feedback models. We use one of their models as a reference model for comparison with this study; Model 1 here

corresponds to Model C of KG03b, which includes cooling and strong SNe feedback.[1] An additional model (Model 2) is constructed, to study the effect of heating by an AGN (see also Springel, Di matteo, & Hernquist , 2004a,b). In Model 2, strong thermal SNe feedback (as in Model 1) is also adopted. In addition, the most bounded star particle in the target galaxy at $z = 1$ is assumed to be the heating source - i.e., the AGN "particle".[2] Since any AGN heating necessarily requires a fuel (gas) source, we assume that the AGN heating is active only when the divergence of the velocity field of the gas surrounding the AGN particle is negative - i.e., $\langle \nabla \cdot \boldsymbol{v} \rangle < 0$. The divergence of the velocity field of the neighbour gas particles is calculated using the SPH scheme. A constant thermal energy of 10^{44}erg s^{-1} is deposited to the neighbour gas particles when the above condition is satisfied. This energy is roughly consistent with observational estimates (e.g. Blanton, Sarazin & McNamara , 2003). The energy is deposited to the neighbour gas particles in the same way as SNe feedback, i.e. smoothed over the neighbour gas particles using the SPH smoothing algorithm (see Sec. 2.3.5 of Kawata & Gibson , 2003a, for details). Hence, we assume that the energy of the AGN heating is distributed spherically in the scale of the smoothing length ($\sim$ kpc) as purely thermal energy. This is obviously too simple, and required to be improved. However, we adopt this simple model for our first study.

We examine both the resulting X-ray and optical properties of the simulation end-products, comparing them quantitatively with observation. The gas particles in our simulations carry with them knowledge of the density, temperature, and abundances of various heavy elements. Using the XSPEC `vmekal` plasma model, we derive the X-ray spectrum for each gas particle, and synthesise them within the assumed aperture. We next generate "fake" spectra with the response function of the XMM EPN detector, assuming an exposure time (40 ks) and target galaxy distance (17 Mpc). Finally, our XPSEC fitting provides the X-ray weighted temperatures and abundances of various elements. In the next section, we compare the simulation results with the X-ray observational data in Matsushita, Ohashi & Makishima (2000, MOM00). MOM00 used the aperture radius of four times the B-band effective radius. The B-band surface brightness profile for our successful model, i.e. Model 2, is barely able to be fitted by the Sersic ($r^{1/n}$) law (Sersic , 1968)[3] , which provides $R_{\mathrm{e},B} \approx 11$ kpc. Hence we applied a projected aperture radius of $R = 45 \approx 4R_{\mathrm{e},B}$ kpc for both models. Conversely, the simulated star particles each carry their own age and metallicity "tag", which enables us to generate an optical-to-near infrared spectral energy distribution for the target galaxy, when combined with our population synthesis code (which itself is based upon the population synthesis models of Kodama & Arimoto , 1997).

3. Discussion and Conclusions

To study both the X-ray and optical properties, we examine the $\mathrm{L_X} - \mathrm{T_X}$ and $\mathrm{L_X} - [\mathrm{Fe/H}]_\mathrm{X}$ relations for the X-ray properties, and the colour-magnitude relation (CMR) for the optical

[1] Thermal energy of 10^{52} erg is applied per supernova, admittedly unrealistic in terms of energetics, but we are only using the model for comparison purposes.

[2] We acknowledge that "turning on" AGN heating at redshift z=1 "misses" the peak of AGN activity in the Universe by $\sim$2 Gyr; our choice of z=1 for this particular model was not driven by empirical cosmological AGN activity arguments, but by identifying the redshift for this model at which a stable "nucleus" could be identified. We will explore this limitation in a future study.

[3] As mentioned in KG03b, the B-band surface brightness profile for Model 1, i.e. Model C in KG03b, is too much centrally concentrated due to the continuous star formation at the centre, and cannot be fitted by the Sersic law.

properties, following KG03b. Throughout this paper, we normalise all abundances to the solar "meteoritic" values from Anders & Grevesse (1989). Fig. 1 show the $L_X - T_X$ and $L_X - [Fe/H]_X$ relations and the CMRs for Models 1 and 2 at $z = 0$, compared that observed. Recall, Model 1 corresponds to Model C of KG03b; such models are broadly consistent with the empirical X-ray properties of ellipticals and agreement driven primarily by radiative cooling (see also Fujita, Fukumoto & Okoshi , 1996; Pearce et al. , 2000).

KG03b showed that radiative cooling ensures that the hot dense gas turns into the cold (i.e. non-X-ray-emitting) gas, and keeps X-ray-emitting gas high temperature and low density. KG03b also found that stars preferentially enrich the gas in the central region where radiative cooling is efficient. The high-density cold gas is incorporated into future generations of stars, and thus a large fraction of the iron ejected from stars is locked into future generations of stars. As a result, the hot gaseous halo which emits X-rays is not enriched efficiently, leading to the lower $[Fe/H]_X$ for Model 1. Hence, radiative cooling ensures that the hot gas has a lower metallicity than the stellar component. However, the optical colours of the resulting stellar component for this model are inconsistent with the observational data (Fig. 1), due to the excessive star formation at low redshift (Fig.) being driven by radiative cooling (see KG03b for more details).

In contrast, the new AGN heating model (Model 2) roughly reproduces both the X-ray and optical observational data. The shaded area in Fig. 1 displays the range of L_X and T_X for a sample of elliptical galaxies with low-L_X and high-T_X (group 5 in MOM00), and 90 % confidence limit of $[Fe/H]_X$ from the composite X-ray spectrum of these galaxies. The X-ray properties for Model 2 are consistent with those for the sample ellipticals. In addition, Fig. 1 demonstrates that the colour and magnitude for Model 2 are consistent with the CMR of the Coma cluster ellipticals and roughly reproduce those for NGC 3923[4] which is the brightest galaxy in this sample.

Of greatest importance for the analysis here is the fact that this AGN heating is sufficiently efficient to suppress the late-time star formation which plagued our earlier study (KG03b). Fig. 2 demonstrates this graphically. As a result, Model 2 succeeds in reproducing - *simultaneously* - both the X-ray and optical properties[5] observed in nearby ellipticals such as NGC 3923. It is also worth noting that the lower $[Fe/H]_X$ in Model 2 is induced by a different mechanism, i.e. blowing out the enriched gas, from that in Model 1, i.e. radiative cooling, because the iron ejected from stars is no long able to be hidden in the cold gas or future generations of stars in Model 2. In fact, we found that compared with Model 1, a larger fraction of iron ejected from stars is blown out from the system by the AGN heating.

Fig. 3 shows the histories of the feedback energy from SNe II, SNe Ia and the AGN. Until star formation ceases at $z \approx 0.4$, the heating due to SNe II is comparable to that of the AGN. However, once star formation stops, the number of SNe II drops, and consequently they become unimportant as a heat source. Conversely, the AGN provides continuous heat to the gas, as

[4] NGC 3923 is known as a shell elliptical. However, their X-ray properties seem to be normal, and old stellar population is dominant (e.g. Michard & Prugniel , 2004). Note that the effective radius of NGC 3923 ($R_{e,B} \sim 6.6$ kpc) is smaller than that for Model 2, which might affect the comparison of the X-ray properties, because we adopted the aperture radius of $4R_{e,B}$.

[5] Fig. 2 shows that Model 2 also reproduces the Type Ia SNe rate observed in nearby ellipticals (Caperrallo, Evans & Turatto , 1999) within the associated observational uncertainties.

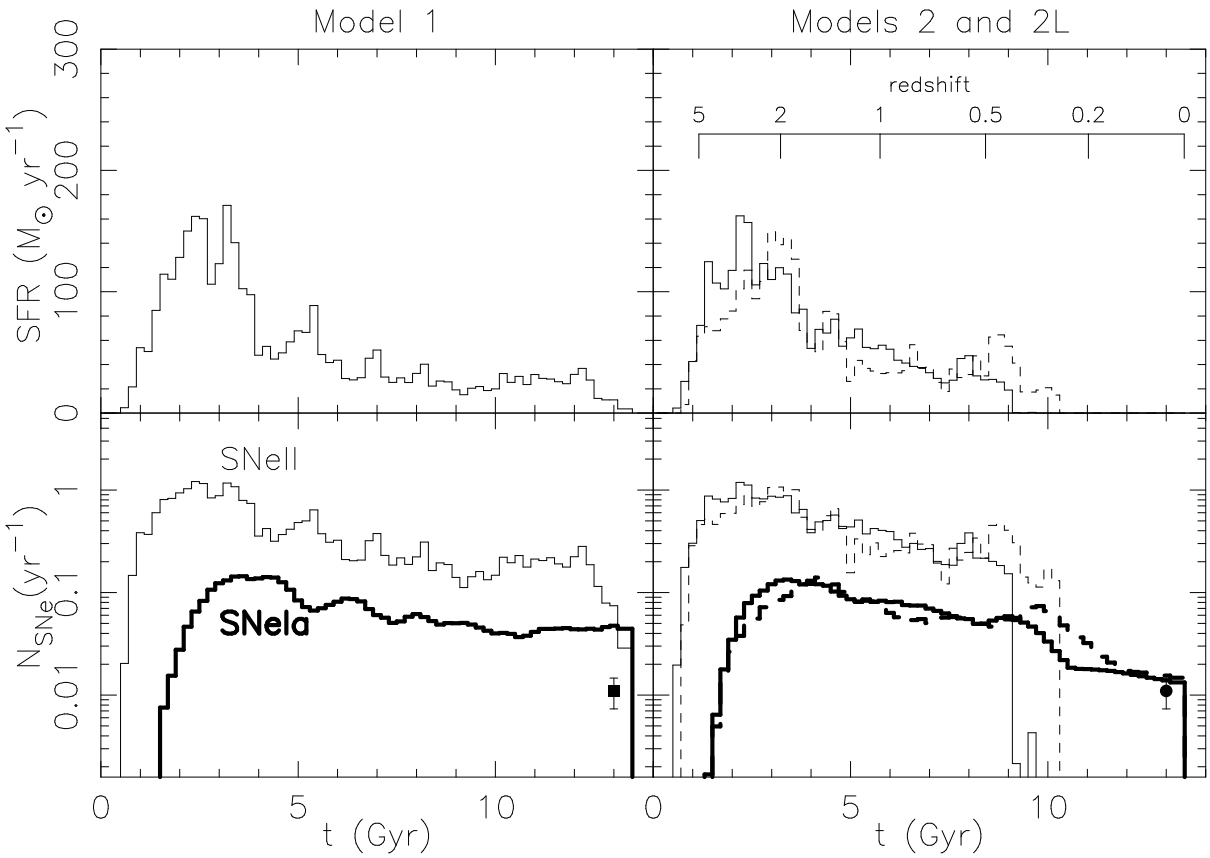

Fig. 2: Time variation of the star formation rate (upper) and the event rate of SNe II (thin lines) and SNe Ia (thick line) for Models 1 (left panels), 2 (solid lines in right panels), and 2L (dashed lines in right panels). Solid square (circle) with error-bar in lower left (right) panel is taken from the observational SNe Ia rate by Caperrallo, Evans & Turatto (1999), taking into account the B-band luminosity for Model 1 (2). To show them clearly, those SNe Ia rates are plotted at t = 13 Gyr.

the AGN activity is not directly linked to the star formation well outside the nucleus. SNe Ia heating by itself is too inefficient to prevent the gas from cooling and subsequent star formation occurring in Model 1. The mean heating energies from SNe Ia and the AGN over the final 3 Gyr of the simulation are 4.8×10^{42} and 2.5×10^{43} ergs, respectively. The efficient, star formation-independent, heating provided by the AGB is required to suppress late-time star formation and, consequently, recover the red stellar populations of ellipticals.

Even after star formation ceases at $z \approx 0.4$, the AGN activity becomes more sporadic, because the gas fueling is also suppressed by the AGN heating itself.[6] This self-regulation of the AGN activity ensures that the hot gas present is not entirely removed from the system due to over-

[6] Note that our assumed AGN heating energy is 10^{44} erg s^{-1}. Hence, in Fig. 3, AGN heating energy of less than 10^{44} erg s^{-1} means that the AGN activity has been "switched on and off" within the period of the size of that bin. This is admittedly unrealistic, as the bin size is small (typically $\sim$ 40 Myr), compared to the typical lifetime of the AGN activity ($\sim$100 Myr). This is a current limitation of the phenomenological AGN model employed.

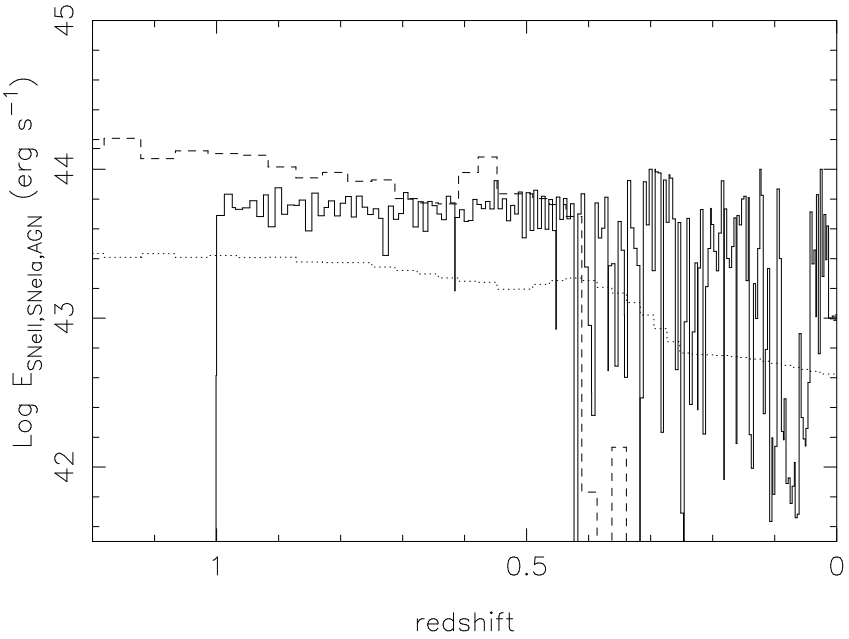

Fig. 3: Histories of the feedback energy from Type II SNe (dashed), Type Ia SNe (dotted) and the AGN (solid), for Model 2.

heating, or entirely converted to cold gas by efficient radiative cooling. For comparison, we also ran a model in which the AGN was continuously active (from redshift z=1 to the present-day) independent of gas kinematics in the central region. We found that such continuous heating blows out the gas from the system completely because of the efficient (and uninterrupted) heating.

Fig. 4 displays the time variation of the relevant X-ray properties for our simulated elliptical galaxies. Here, T_X and $[Fe/H]_X$ are calculated by taking the mean values weighted by $\rho^2 T^{1/2}$ for the gas with $T > 10^6$ K, following Fig. 12 of KG03b. Prior to the cessation of star formation (at $z\approx$0.4), the X-ray properties for Model 2 vary sporadically, but settle into relevant stability thereafter. We suspect that this may be traced to our (too simple) assumption that the AGN becomes active instantaneously at z=1; recall that this heating source was introduced when the simulation was dynamically stable and in possession of a deep potential well. As such, there was a finite time ($\sim$2–3 Gyr) before the AGN could contribute sufficiently to the heat of the surrounding ambient ISM and a new stable configuration reached. In reality, of course, it is likely that the AGN develops before the host system becomes stable, and the AGN heating could affect the hot gas more efficiently. In that picture, we can anticipate the hot gas properties evolving more passively prior at z>0.4, in contrast with the current models. Unfortunately, at this time, it is difficult to construct a more self-consistent model using three-dimensional cosmological hydrodynamical simulations. Nevertheless, our simple model demonstrates that the AGN heating induced by gas infall leads to a stable condition for a lengthy period of time due to its self-regulated nature. Hence, our results shown in this paper are not ephemeral, but represent stable, long-term properties of the simulated ellipticals.

After the hot gas properties reached a stable condition, the X-ray properties are still varying

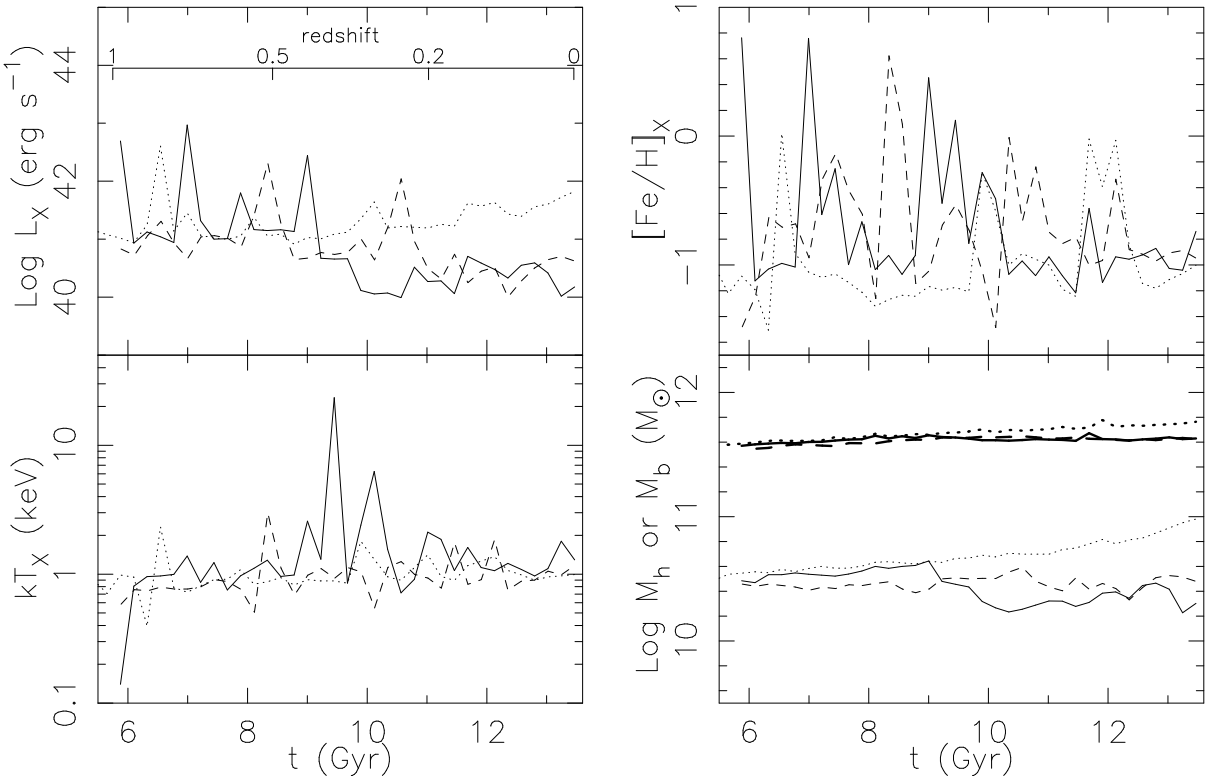

Fig. 4: Time variation of the X-ray luminosity (upper left), temperature (lower left), iron abundance (upper right) and the hot (thin lines) and total baryon (thick line) mass (lower right) within $R = 45$ kpc. The values obtained in Models 1, 2, and 2L are presented as dotted, solid, and dashed lines, respectively.

a little. This temporal variance is considered to represent the range of uncertainties in our simulation[7] . Thus, Fig. 4 means that our simulation cannot tell any difference in T_X or $[Fe/H]_X$ between Models 1 and 2. Conversely, the difference in L_X is significant. The range of $Log(L_X)$ since $z = 0.2$ ($t \approx 11$ Gyr) is 41.2−41.8 and 40.0−40.7 for Models 1 and 2, respectively. Consequently, the AGN heating model reduces the X-ray luminosity for the target galaxy by at least a factor of five, and leads to the X-ray properties similar to low-L_X and high-T_X ellipticals . It would be interesting to examine whether AGN heating can produce the other type of elliptical galaxies, such as high-L_X ellipticals, because it seems that there is no difference in optical properties between low-L_X and high-L_X ellipticals (Kodama & Matsushita , 2000).

Finally, to demonstrate the uncertainty by the numerical resolution, we carried out a simulation (Model 2L) in which the high-resolution region (Sec. 2) consists of lower-resolution particles (27/64 by mass), and the same parameters as Model 2 are adopted. Note that Model 2L has a different pattern of density fluctuations in the high-resolution region, which leads to a different minor merger history from Model 2. Fig. 1 shows that Model 2L provides similar X-ray properties to Model 2 within the range of the temporal variance seen in Fig. 4, i.e. this variance corresponds to the uncertainties of our simulation as described above. Star formation

[7] Some features like a periodic change of L_X in Model 2 seem to be real, because it is caused by the expansion and re-collapse of the hot gas due to the self-regulated AGN activity. However, we postpone such discussion until higher resolution simulations become available.

is quenched by the AGN heating at $z \sim 0.3$ (Fig. 2), and the red colour is reproduced (Fig. 1). Hence, our conclusion shown above is less sensitive to the numerical resolution.

Our cosmological simulation with the AGN heating has successfully produced a system which is consistent with observed elliptical galaxies in both the X-ray and optical regimes. To our knowledge, this is the first elliptical galaxy model which does so *self-consistently*. We admit that our AGN model is rather simple and our study limited by its focus upon only one (representative) elliptical galaxy simulation. Nevertheless, we believe that this encouraging result provides additional impetus for galactic astronomy community to further explore the role that AGN heating plays in the formation and evolution of elliptical galaxies.

参考文献

Anders E., Grevesse N., 1989, Geochim. Cosmochim. Acta, 53, 197

Bertschinger E., 2002, ApJS, 137, 1

Binney J.J. & Tabor G. 1995, MNRAS 276, 663

Blanton E.L., Sarazin C.L., McNamara B.R. 2003, ApJ 585, 227

Bower R.G., Lucey J.R., Ellis R.S., 1992, MNRAS, 254, 589

Böhringer H., Voges W., Fabian A.C., Edge A.C., Neumann D.M., 1993, MNRAS, 264, L25

Brighenti F., Matthews W.G., 1999, ApJ, 515, 542

Cappellaro E., Evans R., Turatto M., 1999, A&A, 351, 459

Churazov E., Brüggen M., Kaiser C.R., Böhringer H., Forman W., 2001, ApJ, 554, 261

Churazov E., Sunyaev R., Forman W., Böhringer H., 2002, MNRAS, 332, 729

Ciotti L., Ostriker J.P., ApJ, 2001, 551, 131

de Vaucouleurs G., de Vaucouleurs A., Corwin H. G., Buta R. J., Paturel G., Fouque P., 1991, Third Reference Catalogue of Bright Galaxies (New York: Springer-Verlag)

Fujita Y., Fukumoto J., Okoshi K., 1996, ApJ, 470, 762

Fujita Y. et al., 2002, ApJ, 575, 764

Kawata D., Gibson B.K., MNRAS, 2003, 340, 908

Kawata D. & Gibson B.K. 2003b, MNRAS 346, 135 (KG03b)

Kodama T., Arimoto N., 1997, A&A, 320, 41

Kodama T., Matsushita K., ApJ, 539, 149

Matsushita K., Ohashi T., Makishima K., 2000, PASJ, 52, 685 (MOM00)

McNamara B.R. et al., 2000, ApJL, 534, L135

Michard R., Prugniel P., A&A, 2004, 423, 833

Pearce F.R., Thomas P.A., Couchman M.P., Edge A.C., 2000, MNRAS, 317, 1029

Persson S.E., Frogel J.A., Aaronson M., 1979, ApJS, 39, 61

Sersic J.-L., 1968, Atlas de Galaxieas Australes (Cordoba: Observatorio Astronomico)

Suginohara T., Ostriker J.P., 1998, ApJ, 507, 16

Springel V., Di Matteo T., Hernquist L., 2004b, ApJL submitted (astro-ph/0409436)

Springel V., Di Matteo T., Hernquist L., 2004b, MNRAS submitted (astro-ph/0411108)

Tornatore L. et al., 2003, MNRAS, 342, 1025